Ultrasound in Med. & Biol., Vol. 23, No. 1, pp. 41–45, 1997

0301-5629/97 $17.00 + .00

ELSEVIER

PII S0301-5629(96)00186-X

●*Original Contribution*

NON-GAUSSIAN STATISTICAL PROPERTY OF THE ULTRASONIC DOPPLER SIGNAL DOWNSTREAM OF A SEVERE STENOSIS

ISABELLE FONTAINE, GUY CLOUTIER and LOUIS ALLARD
Laboratory of Biomedical Engineering, Institut de Recherches Cliniques de Montréal, Montréal, Québec, Canada

(*Received* 2 *April* 1996; *in final form* 13 *August* 1996)

Abstract—The Doppler signal is generally considered as a Gaussian random process. However, to date very little experimental validation of this model has been available. Recently, the K model was proposed to describe the statistical properties of ultrasonic radio frequency signals and their envelopes. The coefficient of kurtosis, which has been shown to be related to the parameters of the K model, was used in the literature as an index to assess the deviations from the Gaussian statistical property of ultrasonic signals obtained from simulations, phantoms and tissues. In the present study, an *in vitro* flow loop model was used to evaluate the effect of a severe stenosis on the coefficient of kurtosis. Our results showed non-Gaussian statistical properties of the Doppler signal in the jet of the stenosis. Copyright © 1997 World Federation for Ultrasound in Medicine & Biology.

Key Words: **Acoustic backscattering, Tissue characterization, Erythrocytes, Statistics, Coefficient of kurtosis, Blood flow, Stenosis.**

INTRODUCTION

The statistical analysis of the speckle pattern of ultrasound B-mode images has been proposed to characterize tissues (Shankar et al. 1993; Tuthill et al. 1988; Wagner et al. 1983). Recently, statistical models of the raw radio frequency (RF) ultrasonic signal and B-mode images were proposed (Chen et al. 1994; Dutt and Greenleaf 1994; Molthen et al. 1995; Narayanan et al. 1994; Weng et al. 1991). The RF ultrasonic signal is generally described by the Gaussian model and its envelope, from which the B-mode image is produced, by the Rayleigh distribution. It was reported in these last studies that there must be a high density of scatterers having identical cross-sections to assume the normality of the RF signal and the Rayleigh characteristics of the echo envelope. In some cases, this condition is not met, as observed in benign or malignant growth, or in abnormal tissues with tumors, where strong isolated scatterers are present.

The K distribution was proposed to describe the non-Rayleigh statistical property of the RF signal envelope (Weng et al. 1991). In the K distribution, the effective number of scatterers (M) is a function of the actual number of scatterers (N) and their cross-sections. More precisely (Shankar et al. 1993):

$$M = N(\gamma + 1), \gamma > -1, \tag{1}$$

where γ represents the lack of uniformity of the scattering cross-sections. Equations associating the normalized statistical fourth moment α_4 with the parameter M of the K distribution were developed (Chen et al. 1994; Weng et al. 1991). When computed from the temporal ultrasonic signal:

$$\alpha_4 = \frac{m_4}{(m_2)^2} = 3\left(1 + \frac{1}{M}\right), \tag{2}$$

while

$$\alpha_4 = 2\left(1 + \frac{1}{M}\right), \tag{3}$$

when evaluated from the envelope of the signal. In

Address correspondence to: Dr. Guy Cloutier, Experimental Ultrasonography and Biorheology Unit, Laboratory of Biomedical Engineering, Institut de Recherches Cliniques de Montréal, 110 avenue des Pins Ouest, Montréal, Québec, Canada, H2W 1R7. E-Mail: cloutig@ircm.umontreal.ca

eqns (2) and (3), α_4, also known as the coefficient of kurtosis, is the ratio of the fourth moment m_4 of the statistical distribution to the square of the second moment m_2.

When the scattering conditions are such that the temporal ultrasonic signal is described by a Gaussian distribution, the parameter M is very large, as expected by the central limit theorem, and α_4 converges toward a value of 3 [see eqn (2)]. However, a low density of scatterers or nonuniform scatterer sizes will result in a deviation from the Gaussian model and a value of $\alpha_4 > 3$.

METHODS

The coefficient of kurtosis α_4 was evaluated on Doppler signals recorded downstream of a severe stenosis. Data from a series of nine experiments collected by Cloutier et al. (1996) were reanalyzed in the present study. For each experiment, the coefficient of kurtosis of the in-phase Doppler signals was computed using the following equation:

$$\alpha_4 = \frac{m_4}{\sigma^4}, \quad (4)$$

where m_4 and σ are the fourth moment and the standard deviation of the statistical distribution, respectively. Considering x_j as the samples of the Doppler signal and N_p the total number of points, m_4 was computed as:

$$m_4 = \frac{\sum_{j=0}^{N_p} (x_j - \mu)^4}{N_p}, \quad (5)$$

where μ is the mean value of the Doppler signal (≈ 0).

As shown in Fig. 1, an acrylic 86% area reduction concentric stenosis was positioned inside a 1.27-cm diameter Kynar tube to produce velocity variations and turbulence downstream of the constriction. The length of the acrylic stenosis was 6.7 cm, and its tapering inlet distance was 1.2 cm ($\theta = 17°$). Doppler measurements were performed with a 10-MHz pulsed-wave system under steady flow. Calf red cells suspended in a saline solution at 40% hematocrit were circulated in the model. All Doppler recordings were performed at the center of the tube using a sample volume of 2.9 mm^3 and a pulse repetition frequency of 39 kHz. Doppler signals were digitized at a rate of 39 kHz over a period of 5 s [N_p in eqn (5) = 195000]. The Doppler angle was maintained at 69° for all measurements obtained by moving the transducer horizontally. The distance between the tip of the transducer and the sample volumes was constant (8.8 mm) for all measurements. One measurement was taken before the stenosis, and a series of 26 other recordings were performed at distances varying between 0.2 and 10.0 D downstream of the stenosis, where D represents the diameter of the nonobstructed section of the tube. The Reynolds number before the stenosis, averaged over nine experiments, was 633 ± 42. Mean velocities within the Doppler sample volume ranging from 40–300 cm/s were measured as a function of the position along the tube.

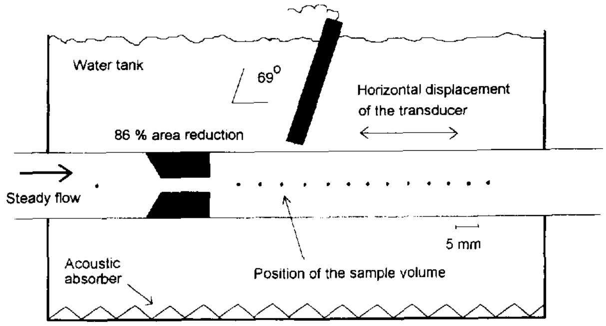

Fig. 1. Schematic representation of the flow model used to determine the centerline axial variation of the coefficient of kurtosis of the Doppler signals.

Statistical analyses

To determine the non-Gaussian statistical property of the experimental data, control values of the coefficient of kurtosis were simulated using the following procedure. Gaussian distributed random signals with $9 \times N_p$ samples were simulated using the "randn" function of Matlab (The Math Works Inc., Natick, MA, USA). The simulated signals were then subdivided into nine segments, each segment corresponding to one experiment of N_p samples. The coefficient of kurtosis was determined using eqn (4).

One-way repeated measures analysis of variance using Bonferroni's method for multiple comparisons (SigmaStat statistical software, Jandel Scientific, San Rafael, CA, USA) was used to assess the differences between the experimental values of the coefficients of kurtosis and the simulated control values. A significance level of 5% was used in all analyses. All results are expressed as mean ± 1 standard deviation (SD).

RESULTS

Figure 2 presents the coefficient of kurtosis as a function of the position along the tube (filled circles). The mean velocities within the Doppler sample volume at each position are also indicated (open circles). Be-

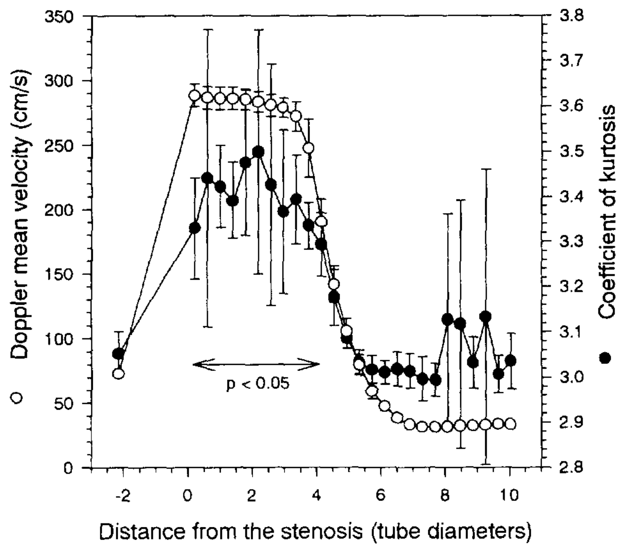

Fig. 2. Coefficient of kurtosis of the Doppler signal (●) and mean velocity within the Doppler sample volume (○) as a function of the position from the 86% area reduction stenosis. All measurements repeated over nine experiments were performed at 40% hematocrit and are expressed as mean ± 1 SD. The analysis of variance was performed between the experimental data and the simulated values of the coefficient of kurtosis (3.00 ± 0.01).

fore the stenosis, the coefficient of kurtosis had a mean value of 3.05, which is similar to the simulated levels of 3.00 ± 0.01. Downstream of the constriction, the values increased up to 3.5 and then decreased to approximately 3.0. Statistically significant differences were obtained between the simulation and the experimental data for distances between 0.2 and 4.2 *D* downstream of the constriction. Between 8 and 9.2 *D*, some fluctuations of the coefficient of kurtosis were noted, but no statistical difference was observed. To better characterize the relationship between the Doppler velocity and the coefficient of kurtosis along the tube, a linear regression was performed. A correlation (r) of 0.74 was obtained, suggesting a dependence between both measurements.

DISCUSSION

To validate the normality of the Doppler signal, the chi-square (χ^2) test was evaluated on simulations (Mo and Cobbold 1986), in experimental laminar and turbulent flow conditions using human red cell suspensions (Bascom et al. 1988, 1993) and on *in vivo* cardiac data (Guo et al. 1993). Important requirements are necessary to use the χ^2 test for determining the non-Gaussian property of signals. For instance, the data must be stationary, and the samples independent and in sufficient quantity (Guo et al. 1993). In practice, it may be difficult to achieve all these requirements. It was shown for continuous-wave (CW) Doppler signals under steady flow that different time window durations can lead to contrary results of the χ^2 test (Bascom et al. 1993). Based on our own experience (Guo et al. 1993), over-sampling of the data can also lead to conflicting results because of the higher statistical dependence between samples. For these reasons, the coefficient of kurtosis was used in the present study as an alternative to the χ^2 test.

Immediately downstream of a severe stenosis (75% area reduction or more), a jet characterized by high red cell velocities is present, and a turbulence zone appears several diameters after the constriction, near the reattachment point of the jet (Jones 1985). As shown in Fig. 2, the coefficients of kurtosis α_4 were maximum in the high velocity jet (between 0.2 and 4.2 *D*). To our knowledge, no study reported results on variations of α_4 for the Doppler signal. In studies related to the scattering of RF ultrasonic signals from tissues (Chen et al. 1994; Narayanan et al. 1994; Shankar et al. 1993), the effect on α_4 of the sample volume, transducer characteristics and frequency of the transmitted signal were investigated. In the present study, these parameters were kept constant for all measurements, thus eliminating these factors as possible sources of variation of α_4. Another characteristic of the coefficient of kurtosis is its sensitivity to artifact, because this parameter depends on the fourth moment of the signal. As a consequence, the presence of air bubbles in a flow model should be considered as a possible source of variability of the results.

In the present study, it is very unlikely that air bubbles were a source of variability or the explanation for the increase in the coefficients of kurtosis between 0.2 and 4.2 *D*, because these artifacts, if present, would have affected α_4 in all positions along the tube. To better assess the possible influence of air bubbles on the values of α_4, an additional analysis was performed to characterize the relative temporal fluctuations of the Doppler power as a function of the position along the tube.* Details on the method used to compute this index are provided in the Appendix. As seen in Fig. 3, the relative fluctuations of the Doppler power were relatively low, between 0.2 and 4.2 *D*. Moreover, no clear correlation existed between the variation of α_4 seen in Fig. 2 and the variation of the relative fluctuations, which indicate the absence of any influence of air bubbles on the coefficients of kurtosis. The variation of the relative fluctuations downstream of the stenosis is very intriguing and deserves more attention in future studies.

* The fluctuations of the Doppler power should increase in the presence of air bubbles.

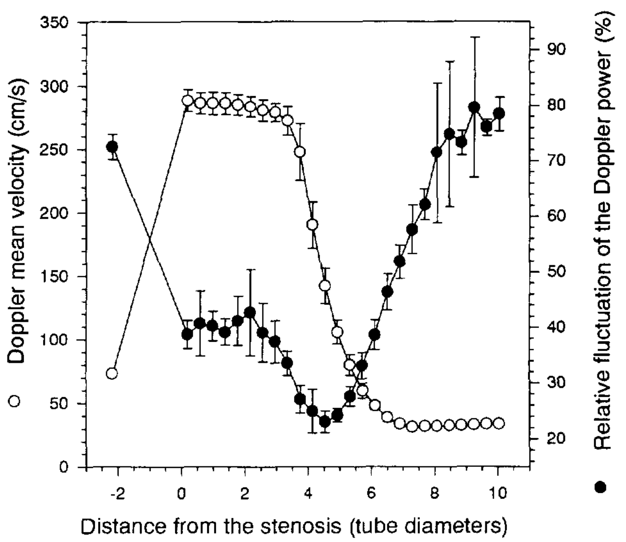

Fig. 3. Centerline axial variation of the Doppler mean velocity (○) and relative fluctuation of the Doppler backscattered power (●) downstream of the 86% area reduction stenosis. The results are expressed as mean ± 1 SD (N = 9 experiments).

As summarized in the Introduction, a low density of scatterers or scatterers with different scattering cross-sections can increase the coefficient of kurtosis. Since the experiments were conducted at 40% hematocrit, the variation of the statistical property of the Doppler signal cannot be attributed to an insufficient concentration of scatterers. It is possible that the acceleration of red cells in the jet and the high velocities of the scatterers caused clustering[*] of the particles, which may have affected the scattering cross-sections [see parameter γ of eqn (1)]. The fluctuations of the effective scattering cross-sections in time and space due to the clustering effect can explain the variations of α_4 in this region.

As observed in Fig. 2, nonstatistically significant increases and large variances of α_4 were measured beyond eight tube diameters. The reasons for these variations are unknown, but they may be related to the presence of turbulence. In a CW Doppler study by Bascom et al. (1988), the statistics of the Doppler signal were affected by turbulence at 28% hematocrit. However, in another study (Bascom et al. 1993), the CW Doppler signal at 42% hematocrit was Gaussian when a short enough time window was used, independently of the position downstream of a 70% area reduction stenosis. In that study, turbulence was observed at approximately five tube diameters downstream of the stenosis. The results from these two studies (Bascom et al. 1988, 1993) performed under steady turbulent flow conditions thus suggest no clear effect of turbulence on the statistics of the Doppler signal. Further investigations are necessary to elucidate the effect of the intensity of turbulence on the coefficient of kurtosis.

CONCLUSION

It was shown in the present study that departure from the Gaussian statistical model can be found for the Doppler signal recorded in the jet of a severe stenosis at 40% hematocrit. This observation may be of importance for correct modeling of the statistical property of the Doppler backscattered signal (Mo and Cobbold 1986, 1989, 1992; Wang and Fish 1996; Wendling et al. 1992). As described in the methodology, all results were obtained from experiments performed using red cells suspended in a saline solution. Using whole blood at flow conditions favoring the formation of red cell aggregates of different sizes, it is likely that non-Gaussian statistical properties may also occur. Since the coefficient of kurtosis is affected by the non-uniformity of the scatterers, this index may also be sensitive to the presence of thrombi, air emboli and ultrasonic contrast agents. Additional experimentations would be interesting to validate these hypotheses.

Acknowledgements—This work was supported by a summer undergraduate studentship (I. F.) and a research scholarship (G. C.) from the Fonds de la Recherche en Santé du Québec. Financing for this project was provided by grants from the Medical Research Council of Canada (#MA-12491), the Whitaker Foundation, USA, and the Heart and Stroke Foundation of Quebec.

REFERENCES

Bascom PAJ, Cobbold RSC, Routh HF, Johnston KW. On the Doppler signal from a steady flow asymmetrical stenosis model: Effects of turbulence. Ultrasound Med Biol 1993;19:197–210.

Bascom PAJ, Routh HF, Cobbold RSC. Interpretation of power changes in Doppler signals from human blood—*In vitro* studies. Ultrason Symp 1988;2:985–988.

Chen JF, Zagzebski JA, Madsen EL. Non-Gaussian versus non-Rayleigh statistical properties of ultrasound echo signals. IEEE Trans Ultrason Ferroelec Freq Cont 1994;41:435–441.

Cloutier G, Allard L, Durand LG. Characterization of blood flow turbulence with pulsed-wave and power Doppler ultrasound imaging. J Biomech Eng 1996;118:318–325.

Dutt V, Greenleaf JF. Ultrasound echo envelope analysis using a homodyned K distribution signal model. Ultrason Imaging 1994;16:265–287.

Guo Z, Durand LG, Allard L, Cloutier G, Lee HC, Langlois YE. Cardiac Doppler blood flow signal analysis. Part I: Evaluation of the normality and stationarity of the temporal signal. Med Biol Eng Comput 1993;31:237–241.

Jones SA. A study of turbulent flow downstream of a constriction in a cylindrical tube at low Reynolds numbers with emphasis on frequency correlations. Ph.D. thesis. San Diego: University of California. 1985:1–196.

Mo LYL, Cobbold RSC. "Speckle" in continuous wave Doppler

[*] Please note that clustering is not referring to the formation of aggregates, which was prevented by the use of calf red cells washed and resuspended in a saline solution. We are referring here to a movement of the red blood cells favoring them to form "clusters" characterized by no specific intracellular link between red cells.

ultrasound spectra: A simulation study. IEEE Trans Ultrason Ferroelec Freq Cont 1986;33:747–753.
Mo LYL, Cobbold RSC. A nonstationary signal simulation model for continuous wave and pulsed Doppler ultrasound. IEEE Trans Ultrason Ferroelec Freq Cont 1989;36:522–530.
Mo LYL, Cobbold RSC. A unified approach to modeling the backscattered Doppler ultrasound from blood. IEEE Trans Biomed Eng 1992;39:450–461.
Molthen RC, Shankar PM, Reid JM. Characterization of ultrasonic B-scans using non-Rayleigh statistics. Ultrasound Med Biol 1995;21:161–170.
Narayanan VM, Shankar PM, Reid JM, Non-Rayleigh statistics of ultrasonic backscattered signals. IEEE Trans Ultrason Ferroelec Freq Cont 1994;41:845–852.
Shankar PM, Reid JM, Ortega H, Piccoli CW, Goldberg BB. Use of non-Rayleigh statistics for the identification of tumors in ultrasonic B-scans of the breast. IEEE Trans Med Imaging 1993; 12:687–692.
Tuthill TA, Sperry RH, Parker KJ. Deviations from Rayleigh statistics in ultrasonic speckle. Ultrason Imaging 1988;10:81–89.
Wagner RF, Smith SW, Sandrik JM, Lopez H. Statistics of speckle in ultrasound B-scans. IEEE Transactions on Sonics and Ultrasonics 1983;30:156–163.
Wang Y, Fish PJ. Simulating nonstationary in-phase and quadrature Doppler signals using a time-varying impulse response filter. Ultrasound Med Biol 1996;22:529–531.
Wendling F, Jones SA, Giddens DP. Simulation of Doppler ultrasound signals for a laminar, pulsatile, nonuniform flow. Ultrasound Med Biol 1992;18:179–193.
Weng L, Reid JM, Shankar PM, Soetanto K. Ultrasound speckle analysis based on the K distribution. J Acoust Soc Am 1991; 89:2992–2995.

APPENDIX

The following approach was used to compute the relative fluctuations of the Doppler power presented in Fig. 3. The digitized in-phase and quadrature components of the Doppler signals were subdivided into rectangular windows of 2 ms. A time interval of 1 ms separated each window from which a Doppler power spectrum was evaluated using autoregressive modeling and zero padding over 1024 samples. Over the data acquisition of 5 s, a total of 4999 spectra was computed. For each spectrum, the mean power P of the forward and reverse components was evaluated as:

$$P = \frac{1}{N} \sum_{f_k = -PRF/2}^{+PRF/2} P(f_k), \tag{6}$$

where $P(f_k)$ represents the power in a bandwidth Δf = 38 Hz (39 kHz/1024) centered at the frequency f_k, PRF = 39 kHz is the pulse repetition frequency and N = 1024 is the number of samples between $\pm PRF/2$. The relative fluctuation of the Doppler power (RFDP) in percent was computed by:

$$RFDP = \frac{RMS[P']}{\langle P \rangle} \times 100, \tag{7}$$

where P' corresponds to the fluctuating components of the Doppler power, RMS is the root-mean-square mathematical operation and $\langle\ \rangle$ is the time-averaging operation. The fluctuating components P' were obtained by removing the time-averaged value $\langle P \rangle$ from each computed value of the Doppler power. This procedure was repeated for each position along the tube and averaged over nine experiments.